Journal of Power Sources, 43–44 (1993) 733–741

Discharge performance of composite insertion electrodes Analysis of discharges of 50 vol.% Li_3N/TiS_2 electrodes

B. C. Knutz*
Chemistry Department A, Building 207, The Technical University of Denmark, 2800 Lyngby (Denmark)

K. West, B. Zachau-Christiansen and S. Atlung
Department of Physical Chemistry, Building 206, The Technical University of Denmark, 2800 Lyngby (Denmark)

Abstract

The dynamic properties of composite insertion electrodes, i.e., mixed-phase electrodes with solid electrolyte and insertion electrode material, have been studied by modelling and experimental investigations. The developed models describe the coupled transport of chemical diffusion in the insertion phase, ionic migration in the electrolyte phase and charge transfer between the two phases. Experimental investigations were performed on a 50 v/o Li_3N/TiS_2 composite electrode. Constant current discharge curves were analysed by comparing with calculations based on the models. In agreement with theory, the discharge curves vary with the square root of time in the beginning of discharge and thereafter directly proportional to time. However, the linear regions were too short. This seems to be caused by a slow transport of lithium in Li_xTiS_2 at high lithium concentrations.

Introduction

Previously we have developed models for different mixed-phase electrodes [1–3]. In ref. 1 numerical simulations of the dynamics of insertion electrodes with liquid organic electrolytes are described. A main result was that the electrode utilization at high discharge rates is limited by salt depletion in the electrolyte pores. When current is drawn from the electrode, concentration gradients are developed in the pores, eventually leading to local salt depletion at higher discharge current densities. This is a consequence of the simultaneous mobility of cations and anions and of the presence of the solvent. For the same reason, salt depletion may also occur in insertion electrodes based on polymer electrolytes with dissolved salt (for instance poly(ethylene oxide) containing $LiSO_3CF_3$ [4]) or the newly developed quasi-solid polymer-gel electrolytes [5, 6]. The latter are essentially liquid organic electrolytes immobilized in network polymers with polar groups.

Salt depletion can be avoided by using solid ionic conductors, polyelectrolytes or appropriate molten-salt electrolytes. As a common feature, the ionic transport in these 'solvent-free' electrolytes is simply given by Ohm's law, opposed to the 'solvent-based' electrolytes, where transport is governed by the more involved Nernst–Planck equation.

*Author to whom correspondence should be addressed.

0378-7753/93/$6.00

In an effort to exploit the advantage of using 'solvent-free' electrolytes, we have studied solid-state cells based on lithium nitride and titanium disulfide with the configuration:

$$Li|Li_3N|LiSO_3CF_3(PEO)_9|Li_3N+TiS_2 \quad (1)$$

A thin sheet of poly(ethylene oxide) electrolyte is placed between the Li_3N separator and the cathode to improve the interfacial contact between the two phases [7]. A cell with a compact 30 μm TiS_2 cathode was cycled at 170 °C with a utilization of 70% at a current density of 2 mA cm^{-2} [7]. Better cycleability and a lower operating temperature were achieved with a mixed phase 50 v/o Li_3N/TiS_2 cathode. A cell was cycled 600 times at 140 °C with 1.90 mA cm^{-2}, corresponding to a stoichiometric discharge time of 1.13 h. The cycling efficiency during the first 300 cycles was 99.87% and the initial utilization was 85% [8]. In the present work, constant current discharge curves of a similar Li_3N/TiS_2 composite electrode are analysed and compared with model calculations.

Experimental

A cell of type (1) with a 50 v/o Li_3N/TiS_2 cathode was discharged at 160 °C with constant currents varying from about 0.1 to 3.0 mA cm^{-2}. An excess of Li metal (Cerac, 99.9%) was used as anode. The separator electrolyte was a 1.2 mm thick Li_3N single crystal. The thickness of the $LiSO_3CF_3(PEO)_9$ film was 0.075 mm. The cathode was prepared from Li_3N (Ventron) and TiS_2 (Cerac, battery grade) powders. In order to obtain a smaller particle size, the received TiS_2 powder was ground under argon in a ball mill. Li_3N was used without pretreatment. The particle sizes of Li_3N and TiS_2 were estimated by means of an optical microscope to 2–4 and 1–2 μm, respectively. The powders were mixed manually and afterwards compressed under vacuum at 10 t cm^{-2}. The thickness of the cathode was 0.26 mm. This corresponds to a porosity of only 2%, calculated from the amounts of Li_3N and TiS_2. The cell was mounted between spring loaded stainless-steel pistons [7]. Preparation of the cathode and assembly of the cell was done in an argon-filled glove box. During measurements, the cell was placed in vacuum.

To obtain an approximately linear emf relation, as assumed in the theory, the discharges were performed from an initial composition of about $Li_{0.45}TiS_2$ (2.24 V) (see Fig. 1). The emf curve shown in Fig. 1 was measured by linear voltammetry performed on an identical cell. The discharges were terminated at a cell voltage of about 1.70 V. After discharge, the cell was kept at open circuit until the voltage was constant within about 0.1 mV over several hours. The same equilibration procedure was applied after charging to an average composition of about $Li_{0.45}TiS_2$. Equilibration of the cell before discharge was necessary in order to facilitate comparison with theory.

Modelling

The discharge performance of mixed-phase insertion electrodes with 'solvent-free' electrolytes has been modelled in ref. 2 assuming negligible charge-transfer resistance, a linear dependence of the emf curve on the degree of insertion, and a uniform concentration of inserted ions in the insertion phase. The latter assumption requires fast diffusion of the inserted ions or that the insertion material consists of small

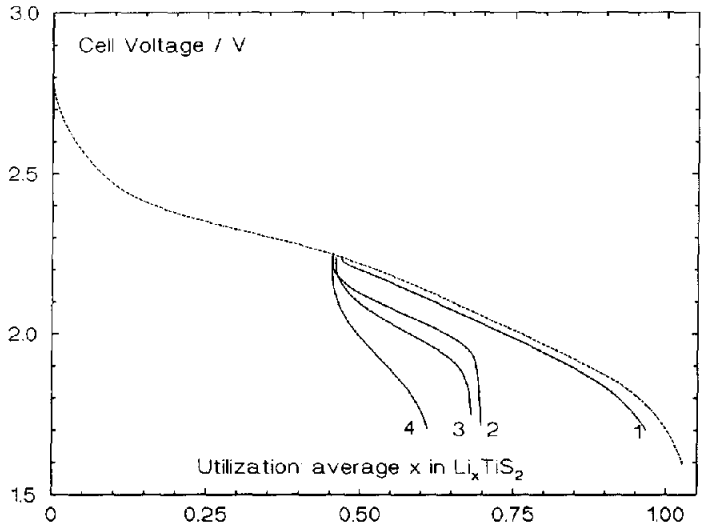

Fig. 1. Emf curve and constant current discharge curves of the cell: $Li|Li_3N|LiSO_3CF_3$-$(PEO)_9|50v/o\ Li_3N+50v/o\ TiS_2$ (160 °C): curve (1) 0.107 mA cm^{-2}; curve (2) 0.950 mA cm^{-2}; curve (3) 1.490 mA cm^{-2}, and curve (4) 3.140 mA cm^{-2}. The emf curve is shown as broken line.

particles [9]. With this condition fulfilled, mixed-phase insertion electrodes with 'solvent-free' electrolytes have been shown [2, 3] to behave as compact insertion electrodes with an enhanced apparent chemical diffusion coefficient, D_c. For a 50 v/o Li_3N/TiS_2 composite electrode the transference number of electrons is close to 1, and D_c is then given by:

$$D_c = \frac{k\sigma_{ci}}{Fvc_{max}} \tag{2}$$

where k is the slope of the linear emf curve, σ_{ci} is the apparent ionic conductivity of the electrode, F is Faraday's constant, v is the volume fraction of insertion material in the cathode and c_{max} is the saturation concentration of inserted ions in the insertion material (also the equations given below are simplified assuming that the electronic conductivity is dominating; general expressions are given in refs. 2 and 10). The improved diffusivity is achieved at the expense of a reduced capacity, vc_{max}!

Due to the assumption of a simple, linear emf relation, analytical solutions of the coupled transport-equations can be derived. With good approximation the discharge curves vary proportional to the square root of time in the beginning of discharge and directly proportional to time after a characteristic transition time, T_t, which is independent of the applied current. The variation of the cell voltage, ϵ, versus time, t, in the two regions can be written as [2]:

$$0 \leqslant t \leqslant T_t \qquad \epsilon(t) = emf_i + RI - k\frac{2}{\sqrt{\pi}}\left(\frac{\tau_c}{\tau_D}\right)^{1/2}\left(\frac{t}{\tau_D}\right)^{1/2} \tag{3}$$

$$T_t \leqslant t \leqslant T_D \qquad \epsilon(t) = emf_i + RI - k\frac{\tau_c}{3\tau_D} - k\frac{t}{\tau_D} \tag{4}$$

where emf_i is the initial equilibrium cell voltage, R is the resistance of the separator electrolyte including charge-transfer resistances at the anode and cathode, I is the current density and T_D is the discharge time. Besides these quantities, the discharge course depends on the time constant of the electrode, τ_c, the stoichiometric discharge time, τ_D, and the transition time, T_t, which are given by:

$$\tau_c \equiv \frac{d^2}{D_c}, \qquad \tau_D \equiv \frac{Fvc_{max}d}{|I|}, \qquad T_t = \frac{\tau_c}{\pi} \tag{5}$$

where d is the electrode thickness.

The $\sqrt{t}$ dependence originates from the fact that the transport of Li in the electrode at the beginning of discharge proceeds as semi-infinite diffusion. At the end of the $\sqrt{t}$ range a parabolic concentration profile has developed. On further discharge, the Li concentration increases uniformly throughout the electrode. Therefore, the shape of the concentration profile remains unchanged and only a linear displacement of the profile occurs with time, giving rise to the linear part of the discharge curve.

In ref. 10, these models are generalized to include the charge-transfer resistance as well as the effects of concentration gradients in the insertion phase assuming a constant diffusion coefficient. Also, in this case a linear discharge range appears for long times. Two additional time-independent overvoltage terms then enter eqn. (4) originating from nonuniform concentration of inserted ions in the insertion particles and from charge transfer between the electrolyte and insertion phase, respectively.

In the general case, the chemical diffusion coefficient will depend on composition, and the emf curve will be nonlinear. For such systems analytical solutions cannot be obtained, and a numerical procedure has therefore been set up to solve the coupled transport-equations [3].

Analysis of experimental results

Generally, both the transport of Li^+ in the electrolyte phase and the chemical diffusion of Li in the insertion particles may limit the discharge performance of the Li_3N/TiS_2 electrode. The rates of these transport processes are given by τ_c and the time constant for chemical diffusion τ_i, respectively ($\tau_i \equiv r^2/\tilde{D}$, where r is the radius of the insertion particles and $\tilde{D}$ the diffusion coefficient). An estimate of τ_c (theoretical lower limit, see below) and τ_i (assuming $r = 2$ μm) for our 50 v/o Li_3N/TiS_2 electrode at 160 °C gives: $\tau_c = 1100$ s, and $\tau_i = 40$ s.

Rather conservatively, $\tilde{D} = 1 \times 10^{-9}$ cm^2 s^{-1}, is assumed [11, 12]. Yet τ_i of the electrode may be larger than 40 s due to agglomeration of the TiS_2 particles and poor contact to the Li_3N particles. Nevertheless, since the estimated value of τ_i is much lower than the estimated lower limit of τ_c, it seems reasonable first to analyse the discharge curves according to the analytical eqns. (3) and (4) assuming chemical diffusion to proceed nearly at equilibrium.

In Fig. 2, the experimental discharge curves are plotted versus $\sqrt{t}$ together with least squares regression lines. In agreement with eqn. (3), the discharge curves are described fairly well by a $\sqrt{t}$ dependence in the beginning of discharge. The presence of a subsequent linear region is demonstrated in Fig. 3. The discharge curves are plotted against the electrode utilization (t/τ_D) together with least square regression lines. No linear range is seen in the discharge curve obtained with 3.14 mA/cm^2, since the discharge time in this case is smaller than the transition time ($T_D < T_t$)!

The slopes and intersections with the ordinate axis of the regression lines are defined in eqns. (6) and (7) and given in Table 1:

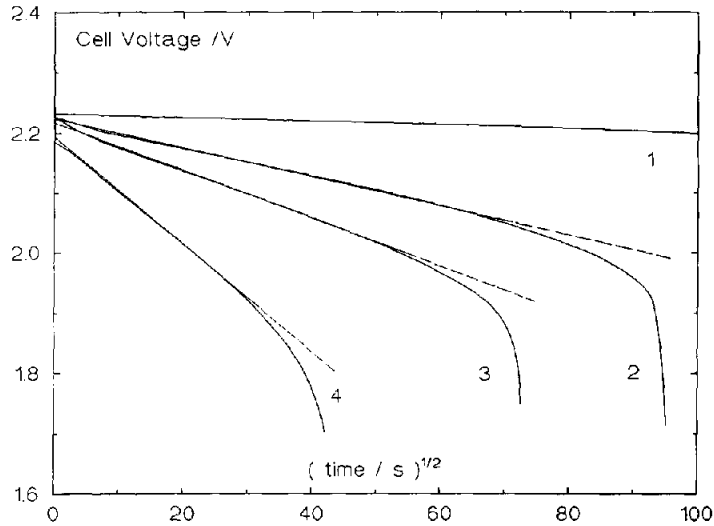

Fig. 2. The experimental discharge curves from Fig. 1 plotted against $\sqrt{t}$ together with least square regression lines: curve (1) 0.107 mA cm^{-2}; curve (2) 0.950 mA cm^{-2}; curve (3) 1.490 mA cm^{-2}, and curve (4) 3.140 mA cm^{-2}. The regression lines are shown broken.

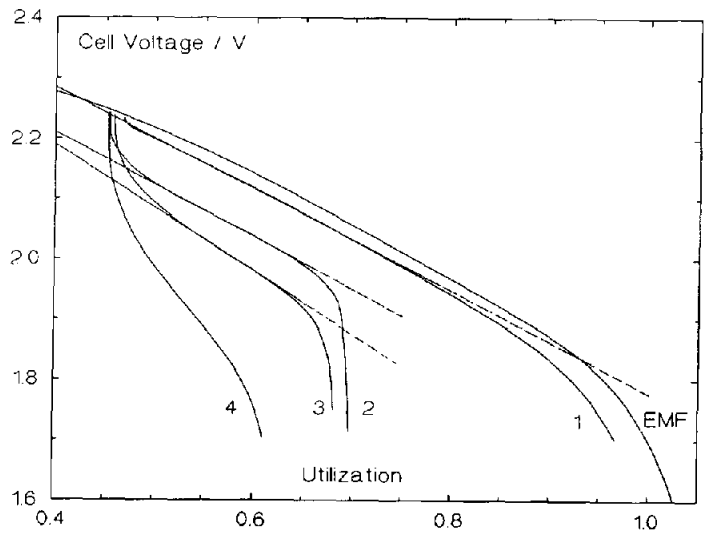

Fig. 3. The emf curve and the experimental discharge curves plotted against utilization (time) together with least square regression lines fitted to the linear part of the discharge curves: curve (1) 0.107 mA cm^{-2}; curve (2) 0.950 mA cm^{-2}; curve (3) 1.490 mA cm^{-2}, and curve (4) 3.140 mA cm^{-2}. The regression lines are shown broken.

Square root region: $\epsilon(t) = A_1 - B_1\sqrt{t}$ (6)

Linear region: $\epsilon(t) = A_2 - B_2 t$ (7)

TABLE 1

Equilibrium voltages, equilibrium degree of insertions and least squares regression parameters belonging to the discharge curves shown in Figs. 1–4

I (mA cm^{-2})	emf_i (V)	emf_t (V)	x_i	x_t	A_1 (V)	B_1 (V s$^{-1/2}$)	A_2 (V)	B_2 (V s^{-1})
0.107	2.2333	1.7951	0.469	0.957	2.2311	2.868×10^{-4}	2.228	2.86×10^{-6}
0.950	2.2425	2.0321	0.454	0.721	2.2189	2.378×10^{-3}	2.163	2.59×10^{-5}
1.490	2.2390	2.0626	0.459	0.687	2.2136	4.073×10^{-3}	2.130	5.01×10^{-5}
3.140	2.2432	2.1180	0.453	0.613	2.1888	9.194×10^{-3}		

A highest possible correlation coefficient was used as criterion for determining the width of the fitting range.

In Table 1 are also given equilibrium voltages before discharge (emf_i) and after discharge (emf_t) and the corresponding equilibrium degree of insertions x_i and x_t, respectively. The latter were obtained by means of the emf curve in Fig. 1.

As seen from eqns. (2)–(4) the time constant of the electrode, τ_c, can be determined from: (i) the slope of the $\sqrt{t}$ plot; (ii) the transition to the linear region, and (iii) the displacement of the linear region of the discharge curve relative to the emf curve. Accordingly, τ_c can be calculated by means of these three expressions:

$$1:\quad \tau_c = \left(\frac{B_1\tau_D\sqrt{\pi}}{2k}\right)^2$$

$$2:\quad \tau_c = \frac{\pi}{4}\left(\frac{B_1}{B_2}\right)^2$$

$$3:\quad \tau_c = \frac{(A_1-A_2)3\tau_D}{k} \qquad (8)$$

The first and last expressions require knowledge of k and τ_D. Linearization of the emf curve for $x \geqslant 0.45$ gives $k = 0.875$ V. Calculating τ_D from eqn. (5) or the weighed amount of TiS_2 would most likely result in too high values, because some of the TiS_2 used in the electrode may be chemically inert or inaccessible for the electrochemical reaction. τ_D was therefore calculated from:

$$x_t = x_i + \frac{T_D}{\tau_D} \qquad (9)$$

The experimental discharge times, T_D, and calculated values of τ_D and τ_c are given in Table 2. The value $\tau_c = 3240$ s is obviously too small. This can, however, be ascribed to a high uncertainty since τ_c in this case is calculated from a very small difference, $A_1 - A_2$. Furthermore, the value 9380 s is relatively high, which can be traced back to a high slope, B_1. This is probably a result of the decrease in Li diffusion in the insertion phase at high degree of insertion, see below. Otherwise, the three different ways of calculation τ_c result in reasonably equal values. This shows that the analytical solutions are quantitatively consistent.

Averaging of the τ_c values (omitting 3240 s) gives $\langle\tau_c\rangle = 7080$ s. From this figure and eqns. (2) and (5) the apparent diffusion coefficient and apparent ionic conductivity

TABLE 2

Parameters derived from the discharge curves in accordance with the analytical solutions

I (mA cm^2)	R^a (Ω cm^2)	k^b (V)	T_D (s)	τ_D (s)	Q^c (C cm^{-2})	1: τ_c (s)	2: τ_c (s)	3: τ_c (s)
0.107	20.6	0.87	148800	305000	32.6	7850	7900	(3240)
0.950	24.8	0.80	8200	30800	29.3	5500	6620	5900
1.490	17.0	1.00	4770	20900	31.1	7430	5190	5990
3.140	17.3		1660	10400	32.7	9380		

[a]Separator electrolyte resistance, $R=(emf_i-A_1)/|I|$.
[b]Slope of emf curve, $k=B_2\ \tau_D$.
[c]Accessible capacity of electrode, $Q=I\ \tau_D$.

of the electrode can be calculated as ($c_{max}=0.0283$ mol/cm^3):

$D_c=9.7\times10^{-8}$ cm^2 s^{-1} $\quad(6.1\times10^{-7}$ cm^2 s$^{-1})$

$\sigma_{ci}=1.5\times10^{-4}\ \Omega^{-1}$ cm^{-1} $\quad(9.8\times10^{-4}\ \Omega^{-1}$ cm$^{-1})$

For comparison, the theoretical maximum values are given in brackets. These figures were calculated based on the ionic conductivity of dense polycrystalline Li_3N taking into account the effect of anisotropic conduction in Li_3N, volume fraction and tortuosity [3, 8, 13]. The discrepancy reflects the difficulty of obtaining good contact between the hard Li_3N particles. Since TiS_2 is a soft layered compound, the contacts between Li_3N particles are probably established through thin films of TiS_2.

Nevertheless, the experimental value of D_c is considerably higher than the chemical diffusion coefficient 3.5×10^{-9} cm^2 s^{-1}, which was measured on compact Li_xTiS_2 electrodes ($x\sim0.64$) at 160 °C using the same cell configuration and TiS_2 powder as in the present work [3]. Thus Li_3N greatly improves the transport of Li in the electrode.

Table 2 also contains experimental values of the separator resistance, emf slope and electrode capacity, Q. As expected, these quantities are reasonably independent of current density. The calculated separator resistances correspond to a separator electrolyte conductivity of $5–8\times10^{-3}\ \Omega^{-1}$ cm^{-1} which is in good agreement with the conductivity of Li_3N [14]. The electrode capacities given in Table 2 should be compared with 35.3 C cm^{-2}, calculated from the amount of TiS_2. The difference indicates that some of the insertion material is isolated in the electrode.

Apart from a small variation in the slope of the linear regions, the major part of the discharge curves are well described by the analytical solutions. However, compared with the linear model the discharges terminate too early giving unexpectedly low utilizations. The last part of the discharges may be dominated by the nonlinear emf curve and the decrease of chemical diffusion of Li in Li_xTiS_2 for $x\rightarrow1$ [11]. The influences of these nonlinearities on the discharge curves were investigated by simulations. It turns out that calculated discharge curves, based on a constant τ_i ($\tilde{D}$) but taking into account the variation of the real emf curve, do not describe the experimental discharges satisfactorily [3]. Only simulated discharge curves, calculated on the basis of a strong decrease in the chemical diffusion coefficient for $x\rightarrow1$, give acceptable agreement with experiment (see Fig. 4). A better description of the experimental discharges than given in Fig. 4 may be possible by optimizing on τ_c and the magnitude and variation of $\tilde{D}$. However, some of the discrepancies are probably due to changes in electrode properties caused by the performed discharges.

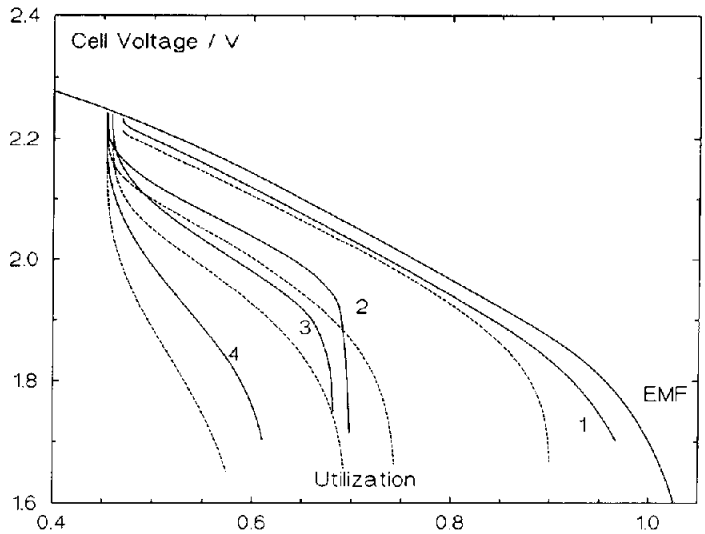

Fig. 4. The experimental discharge curves and simulated curves (shown broken) plotted vs. utilization. The simulated discharges were calculated taken into account the nonlinearity of the emf curve and were based on the following conditions: $\tau_c = 8000$ s, $d = 0.26$ mm, $v = 0.5$, $r = 1.7$ μm (radius of insertion particles) and a variation of the chemical diffusion coefficient of Li in Li_xTiS_2 given by: $\log(\tilde{D}) = -6.67(x-0.5)^2 - 11.33$; curve (1) 0.107 mA cm^{-2}; curve (2) 0.950 mA cm^{-2}; curve (3) 1.490 mA cm^{-2}, and curve (4) 3.140 mA cm^{-2}.

In order to explain the experimental discharges we were led to assume chemical diffusion coefficients $< 5 \times 10^{-12}$ cm^2 s^{-1}. These are considerably lower than the estimated single crystal value (1×10^{-9} cm^2 s^{-1} at 160 °C). This means that the apparent particle size of Li_xTiS_2 in the electrode is much larger than the physical of 1–2 μm, which to some extent is caused by agglomeration of the insertion particles. However, the main reason is probably a poor contact to the Li_3N particles.

Because of the contact problems, soft vitreous electrolytes [15] or polyelectrolytes [16] may be preferable for solid-state batteries compared with ceramic solid ionic conductors, like Li_3N.

Conclusions

The discharges of a Li_3N/TiS_2 composite cathode have been analysed and compared with model calculations. In accordance with theory, the discharge curves vary with good approximation proportional to the square root of time for small times. The discharge curves also show a subsequent linear region. However, compared with the analytical solutions, the experimental discharges drop off too early, possibly due to a decline in chemical diffusion for high Li concentrations. Accordingly, better fits were obtained with discharge curves calculated by means of numerical simulations, taking into account the variations of the chemical diffusion coefficient with the degree of insertion and the nonlinearity of the real emf curve of Li_xTiS_2.

Acknowledgement

The Danish Ministry of Energy is thanked for financial support.

Note added in proof

After preparation of the manuscript, the authors have become aware of a paper by J. R. Akridge *et al.* [17], in which an analysis of the same type as in the present work is performed on a TiS_2/glass composite electrode. The results reported are consistent with the results presented in this paper.

References

1 K. West, T. Jacobsen and S. Atlung, *J. Electrochem. Soc., 129* (1982) 1480.
2 S. Atlung, B. Zachau-Christiansen, K. West and T. Jacobsen, *J. Electrochem. Soc., 131* (1984) 1200.
3 B. C. Knutz, *Thesis*, The Technical University, Lyngby, Denmark, 1985.
4 M. B. Armand, *Ann. Rev. Mater. Sci., 16* (1986) 245.
5 R. Huq, R. Koksbang, P. E. Tønder and G. C. Farrington, in K. M. Abraham and M. Salomon (eds.), *Primary and Secondary Lithium Batteries,* Proc. Electrochemical Society, Pennington, NJ, Vol. 91-3, 1991, p. 142.
6 K. M. Abraham and M. Alamgir, *J. Electrochem. Soc., 137* (1990) 1657.
7 B. C. Knutz and S. Skaarup, *Solid State Ionics, 9/10* (1983) 371.
8 B. C. Knutz and S. Skaarup, *Solid State Ionics, 18/19* (1986) 783.
9 S. Atlung, K. West and T. Jacobsen, *J. Electrochem. Soc., 126* (1979) 1311.
10 B. C. Knutz, S. Atlung, K. West and U. Henriksen, to be submitted.
11 K. Kanahori, F. Kirino, T. Kudo and K. Miyauchi, *J. Electrochem. Soc., 138* (1991) 2216.
12 P. G. Bruce and M. Y. Saidi, *Electrochim. Acta, 36* (1991) 569.
13 R. E. Meredith and C. W. Tobias, *Adv. Electrochem. Electrochem. Eng., 2* (1965) 15.
14 T. Lapp, S. Skaarup and A. Hooper, *Solid State Ionics, 11* (1983) 97.
15 J. R. Akridge and H. Vourlis, *Solid State Ionics, 18/19* (1986) 1082.
16 M. A. Ratner and D. F. Shriver, *Chem. Rev., 88* (1988) 109.
17 J. R. Akridge, S. D. Jones and H. Vourlis, *NATO ASI Ser. B: Phys., 217* (1988) 363.